Earth, Planets and Space

FULL PAPER Open Access

A convolutional neural network to optimize multi-mission satellite altimeter fusion for improving the marine gravity field

Qianqian Li[1], Zhenhe Zhai[2], Lifeng Bao[1,3*], Yong Wang[1,3], Lin Wu[1], Guocheng Mao[1,4] and Heping Sun[1,3]

Abstract

Satellite altimetry is the main tool for constructing global or regional marine gravity fields. To improve the accuracy and spatial resolution, it is necessary to fuse multi-mission altimeters. How to determine the weights of multi-mission altimeters is a crucial issue, making the conventional calculation process very complex. In addition, traditional satellite inversion methods are often independent of shipborne gravity, which is used only as validation data, thus not take full advantages of high accuracy and resolution of shipborne gravity. In this study, we introduce a convolutional neural network (CNN) to merge the vertical deflections (DOVs) obtained from multi-altimeter missions to construct a marine gravity model in the South China Sea. High-accuracy shipborne gravity and a dataset comprising DOVs and geolocations are employed as input data for neural network training. For the validation of CNN method, the gravity model is also computed by conventional Inverse Vening Meinesz (IVM) method. Independent shipborne gravity measurements and SIO V32.1, DTU17 models are used as validation data. The evaluation results show that the CNN-derived model achieves a higher level of accuracy, yielding a standard deviation (STD) of 3.21 mGal, with an improvement of 36.56% compared to IVM-derived model. More than 92% of the differences between the CNN-derived model and shipborne gravity are less than 5 mGal. In addition, spectral analysis results further show that the CNN-derived model has stronger energy at short wavelengths (less than 25 km) compared to other models. These findings reveal that CNN method is feasible for marine gravity recovery and the CNN-derived model can achieve higher accuracy. The CNN method can improve the accuracy and spectral characteristics of the constructed gravity model by taking advantage of the high accuracy and high resolution of shipborne gravity.

Keywords Marine gravity, Convolutional neural network, Satellite altimeter, Vertical deflection, Inverse Vening Meinesz formula

*Correspondence:
Lifeng Bao
baolifeng@whigg.ac.cn
Full list of author information is available at the end of the article

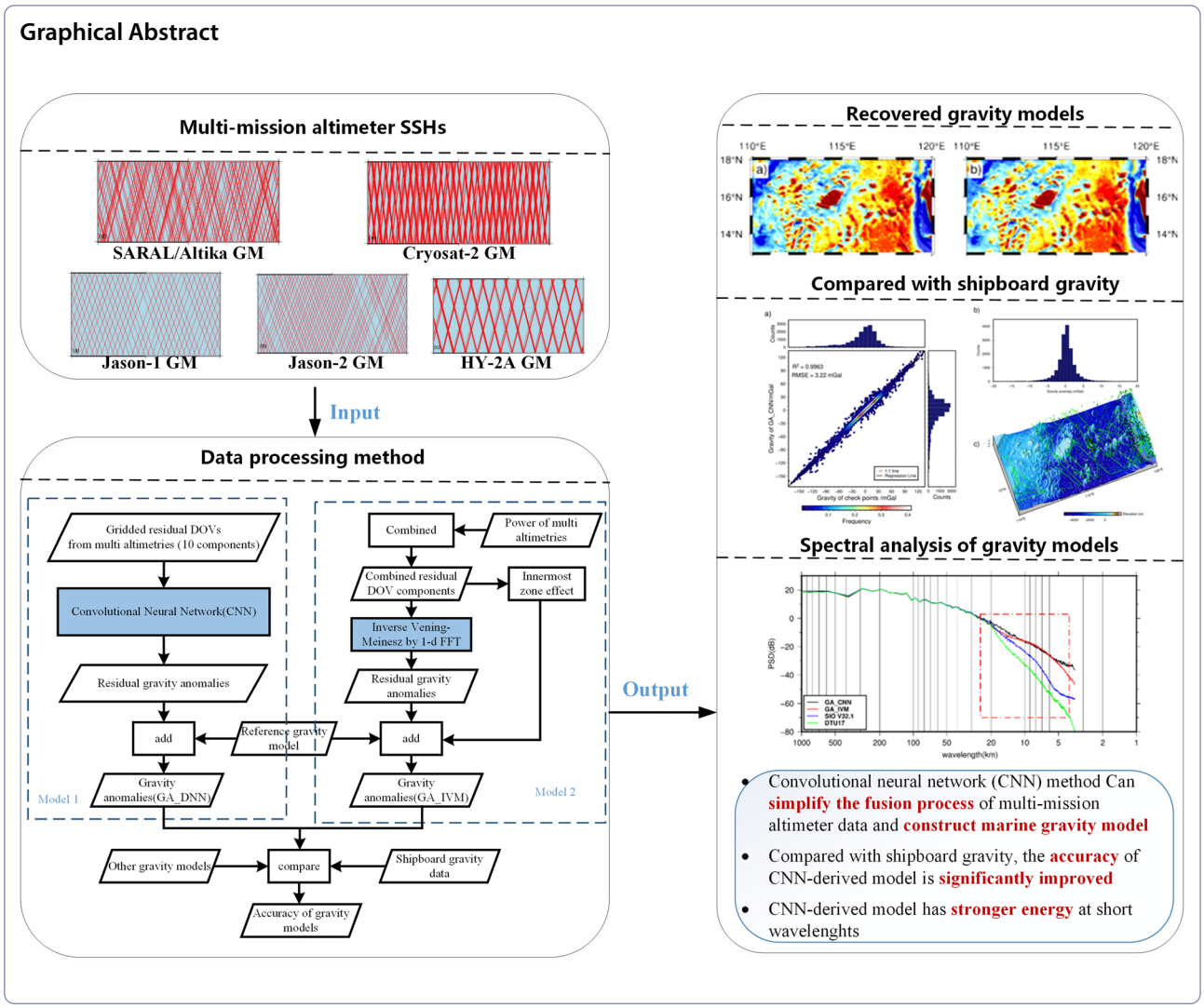

1 Introduction

Marine gravity field serves as the essential data for ocean observations, reflecting the distribution, movement, and density changes of materials under the ocean. Accurate knowledge of marine gravity field is crucial for understanding the distribution of marine resources, submarine topography and tectonics, as well as underwater vehicle navigation, benefiting science and society. Marine gravity can be obtained mainly by satellite altimetry and shipborne gravity measurements. Satellite altimetry can provide rapid access to global sea surface heights (SSHs), and measure the shape of the Earth and the geoid, thereby to obtain the global marine gravity field. Over the past decades, thanks to the accumulation of multi-source altimeter data, satellite altimetry has developed into an essential tool for constructing global or regional marine gravity models (Andersen and Knudsen 1998; Haxby et al. 1983; Hwang 1998; Sandwell and Smith 2009). Shipborne gravity measurements offer advantages in accuracy and resolution, and are an important aid in obtaining marine gravity. At present, to further enhance the accuracy and resolution of marine gravity, it is necessary to maximize the integration of multi-source data, including altimeter data and shipborne gravity measurements, while taking advantage of the strengths of each data.

The spatial track density, range precision and trajectory diversity of altimeter are the primary factors affecting the spatial resolution and accuracy of altimetry-derived marine gravity. Combining multi-mission altimeter data, especially from geodetic missions (GMs), is an effective way to improve the spatial density, trajectory diversity and volume of SSHs (Andersen et al. 2010, 2021; Sandwell et al. 2021; Zhu et al. 2020). Different altimeters have different levels of accuracy. When combining multi-mission altimeter data, how to determine appropriate

weights for each mission to achieve an optimal result is particularly important. It has been an indispensable component in the study of marine gravity recovery.

Sandwell and Smith (1997) applied an a priori estimate of along-track slope error, to weight the Geosat and ERS-1/GM data. Hwang (1998) weighted the altimeter data from Seasat, Geosat ERS-1 and TOPEX/POSEIDON (T/P) based on the standard deviations (STDs) of mean geoid gradients, and derived a global marine gravity model by empirical variances function and remove–compute–restore (RCR) technology. This method has been used to weight multi-source altimeter data, including new GM data from SARAL/AltiKa/Drifting Phase (AltiKa/DP), Cryosat-2, Jason-1/2 and HY-2A since 2010 (Hwang et al. 2002; Yu et al. 2021; Yu and Hwang 2022). Different observation modes and observation bands of the altimeter complicate the weighting strategy. Zhu et al. (2020) proposed a new iterative method to estimate the weight of the Ka-band AltiKa altimeter. Yu and Hwang (2022) employed the theory of minimum norm quadratic unbiased estimator to calibrate the error variances of geoid gradients from Cryosat-2 and Jason-1/2 missions and calculated the gravity field in the Gulf of Mexico. These studies indicate that the process of weights determination and combination of multi-mission altimetry data is very complicated. Moreover, the covariance function sometimes fails to fully reflect the error characteristics of each satellite, the resulting weights do not achieve the optimal results.

The main approaches for marine gravity recovery from multi-mission altimeters include the inverse Stokes integral, the inverse Vening Meinesz (IVM) formula, the Laplace equation, and the least squares collocation (LSC) method. The inverse Stokes integral is appliable for marine gravity recovery from geoid heights (Wang 1999). The IVM method and the Laplace equation depend on vertical deflections (DOVs) as data source (Hwang 1998; Sandwell and Smith 1997). The LSC method is based on statistical theory and can be used for geoid heights or DOVs. This method relies on a precise covariance matrix between the geoid heights or DOVs and the gravity anomalies, which is difficult to determine exactly. So, it has been used relatively infrequently (Andersen and Knudsen 1998; Olgiati et al. 1995). DOVs are the slope of the geoid in the north–south and east–west directions. Theoretically, due to differential computation, DOVs are less contaminated by long-wavelength radial orbit error, while containing more short-wavelength signals, resulting in that IVM and Laplace equation methods are widely used in gravity recovery (Hwang et al. 2002; Sandwell and Smith 2009; Zhang et al. 2021). However, these common traditional methods rely on strict functional relationship between geoid or DOVs and gravity anomalies, and are often independent of shipboard gravity measurements, which are used only as validation data. This simplifies the complex correlational relationship between geoids or DOVs and gravity anomalies and prevents these methods from taking full advantage of the high accuracy and resolution of shipborne gravity. In this study, we attempt to propose a new inversion method, based on neural networks, which using DOVs as data source.

Neural networks are applicable to simplify the process of gravity recovery from multi-source altimeters and shipborne gravity, due to their powerful massive data processing and nonlinear fitting capabilities. They have been successfully applied in seismic detection and location (Perol et al. 2018), noise suppression (Dong et al. 2020; Zhao et al. 2018), and bathymetry prediction (Annan and Wan 2022; Li et al. 2023; Sun et al. 2022). Neural networks can map various geophysical transfer functions and fuse data from multiple sources to accomplish regression tasks efficiently with high accuracy. Convolutional neural network (CNN) is one of the most widely used neural network model, performing well in extracting highly non-linear features from images, which is challenging for traditional physical algorithms. Therefore, it is possible to adopt CNN to recover the marine gravity by combining multi-mission altimeters without complex weight determination.

In this paper, we attempt to construct the marine gravity field in South China Sea (SCS) by CNN method and RCR technology. CNN has been utilized to recover gravity data in the western Pacific Ocean from satellite altimetry data (Zhu et al. 2023). Distinguished from other studies, we focus on the ability of the CNN method to simplify the fusion of multi-satellite datasets. We derive gravity in short waveband from CNN rather than absolute gravity, since altimeter data can improve the short-wavelength gravity field primarily. We also use high-resolution shipborne gravity measurements to assess the actual resolution of the CNN inversion results compared to other models. Specifically, we first calculate multi-source altimetry-derived DOVs from Altika/DP, CryoSat-2, Jason-2/GM, HY-2A/GM, and Jason-1/GM in SCS. Then, we design a CNN using DOVs and geo-locations as input data, and shipborne gravity measurements as training data. The shipborne gravity measurements require quality control and band separation. Finally, we construct a $1' \times 1'$ marine gravity model by the designed CNN and evaluate its accuracy by comparing with conventional IVM method and other gravity data.

2 Study area and data

2.1 Study area

The SCS is located at the junction of the Eurasian plate, Indo-Australian plate, and Philippine Sea plate. As one of the marginal seas of western Pacific, its relatively complex seafloor topography records the formation and evolution of the whole marginal sea, which provides a natural geological laboratory for the study of continental rifting and seafloor spreading processes. SCS is rich in tectonic units, including islands, trenches, basins, and submarine plateaus, and so on (as shown in Fig. 1a). The marine gravity field of SCS is the basic data for crustal structure and tectonic unit research. Therefore, the region of SCS within 13°–18° N, 110°–120° E is selected as the study area to recover the regional marine gravity field using multi-altimeter data sets (Fig. 1a and the red rectangle in the upper right). Considering the edge effect, the region expands outward by 1° during the calculation process (black dashed rectangle in the upper right of Fig. 1a). The region has a large topographic relief, with water depths ranging from 0 to 5000 m. The landforms are characterized by their complexity and diversity, encompassing seamounts, sea basins, trenches, and other features. These characteristics provide a comprehensive validation of the neural network method's efficacy in gravity recovery.

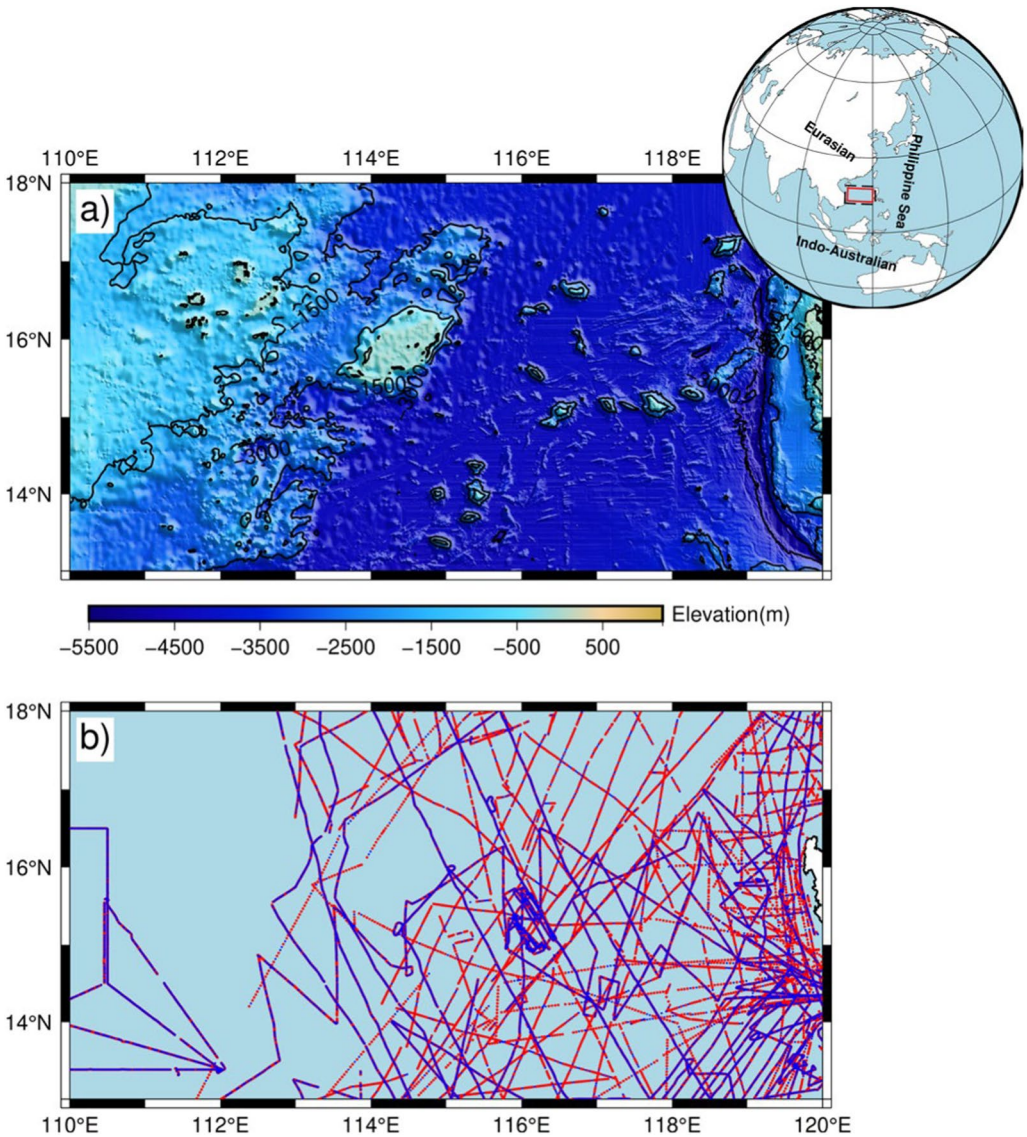

Fig. 1 Bathymetry of the study area (**a**) and the distribution of shipborne gravity. (**b**) Red dots and blue dots in figure b) denote calculate points (which are used for training the neural network) and check points (which are excluded from training), respectively

2.2 Datasets used

2.2.1 Shipborne gravity data

As training sample, the collection of shipborne gravity data is the first priority. The shipborne gravity data used in this study are available from the National Centers for Environmental Information (NCEI) and SeaDataNet. The main types of features we use to train the recovery are longitude, latitude, and free-air gravity anomaly. The free-air anomalies have been adjusted for drift correction, lag time and Eötvös correction. The total number of shipborne gravity points is 80,899, and their distribution is shown in Fig. 1b.

For quality control, it is necessary to edit the shipborne gravity first to remove incorrect measurements (see Sect. 3.1). Then to train a neural network model, approximately 80% (64,720 data points illustrated as red dots in Fig. 1b) are selected evenly as calculate points to train the neural network. These data are processed to get the short-wavelength component. During the training process, 80% of the calculate points is randomly selected as the training set and 20% as the test set to iteratively optimize the model. The remaining data points (16,179 points depicted as blue dots in Fig. 1b) are independent of the calculation process and used as check points to evaluate the altimeter-derived gravity models.

2.2.2 Altimetry data

Up to now, there are several satellite altimeters providing numerous SSHs data of GMs, including Geosat/GM, ERS-1/GM, Jason-1/GM, CryoSat-2, HY-2A/GM, Altika/DP, and Jason-2/GM. Whether all geodetic missions still make great contributions to the marine gravity recovery is a concern for simplifying the gravity construction processes. Sandwell et al. (2021) assessed the contribution of each altimeter GM to the marine gravity recovery, and found that Geosat/GM and ERS-1/GM provide minor improvement. Therefore, SSHs data from Geosat/GM and ERS-1/GM are excluded from this study, and data from Altika/DP, HY-2A/GM, CryoSat-2, Jason-1/GM and Jason-2/GM are employed, and the information on the GMs used are shown in Table 1.

We mainly use the 1 Hz along-track non-time critical Level-2 Plus (L2P) products, which can be accessed through AVISO. The L2P products are results of further processing of Level 2 altimetry data (geophysical data records, GDRs). L2P products for all altimetry missions have a uniform format and content (CNES 2020). The reference datum used is WGS-84, which is similar with shipborne gravity data. For Jason-2/GM, the 1-Hz GDRs in Ku band are adopted due to the less measured SSHs from L2P. GDRs have a different reference ellipsoid with equatorial radius of 6378.1363 km and flattening coefficient of 1/298.257 from that of WGS 84, which should be transformed before calculating the DOVs (Jin et al. 2008; Rapp et al. 1994). In the end, we use the SSHs after data editing and various geophysical corrections.

2.2.3 Dynamic topography model and reference gravity field

Given the effect of sea surface topography, a dynamic topography model is considered to interpolate and remove from altimeter-measured SSHs before calculating DOVs. The mean dynamic topography (MDT) model MDT-CNES-CLS18 from AVISO is employed in this study. MDT-CNES-CLS18 model is an estimate of the mean sea surface height above geoid over the 1993–2012 period, with a global geographic coverage and resolution of 0.125°.

To derive gravity in a certain waveband, RCR technique is introduced to separate the gravity field into the long-wavelength reference field and the short-wavelength residual field (Forsberg 1984). In this study, the Earth Gravitational Model 2008 (EGM2008) is chosen as the reference gravity field, which is one of the widely used combined global gravity field models (Andersen and Knudsen 2019; Pavlis et al. 2012; Sandwell and Smith 2009; Zhang et al. 2017; Zhu et al. 2020). EGM2008 is a spherical harmonic model of the Earth's gravitational potential, which is completed to degree and order 2159, and contains additional coefficients up to degree 2190 and order 2159 (Pavlis et al. 2012). By removing the MDT-CNES-CLS18 model and EGM2008-derived geoid from the SSHs, residual geoid heights can be obtained, which are the key data for DOVs calculation.

Table 1 Information of altimeter data used in this study

Satellite	Product	Time scope	Cycle scope	Orbit inclination	Repeat cycle (d)	Cross-track distance at equator (km)
Altika	L2P	16.07–23.07	100–173	±81.5	–	~5
CryoSat-2	L2P	10.07–20.05	007–130	±88	369	~2.5
HY-2A	L2P	16.03–20.05	118–288	±81	168	~15
Jason-1	L2P	12.05–13.06	500–537	±66	406	~7
Jason-2	GDR	17.07–19.10	500–644	±66	369	~7

2.2.4 Gravity data for validation

To evaluate the accuracy of marine gravity models using external data is an important part of marine gravity recovery. The models of V32.1 from Scripps Institution of Oceanography (SIO), DTU17 from DTU space (DTU) are introduced to verify the recovered gravity model. They adopted different multi-satellite altimeter dataset and data processing method that ensure independence from recovered model. SIO V32.1 adopted new altimeter data from Envisat, Cryosat-2, Jason-1/2, Altika and Sentinel-3A/B. Advanced data processing methods such as retracking waveforms, slope correction, biharmonic spline interpolation, multiple filtering, and Laplace equation are employed for gravity recovery. As a result, it has a spatial resolution up to $1' \times 1'$ and an accuracy up to 1–2 mGal in some regions (Sandwell et al. 2014, 2021). DTU17 employed the altimeter data from Geosat, ERS-1, Cryosat-2, Jason-1 and Altika, which have been processed with double waveform retracking method to improve the range accuracy, especially in coastal and polar regions. And it calculated the marine gravity by inverse stokes formula from altimeter measured geoid (Andersen and Knudsen 2019). It is widely recognized that these marine gravity models have high spatial resolution and accuracy, and are typical marine gravity models in the world, which are used as a comparative standard for accuracy assessment.

3 Methods

In this study, the altimeter-measured SSHs after geophysical correction obtained from satellite missions such as Altika/DP, CryoSat-2, Jason-2/GM, HY-2A/GM and Jason-1/GM are used. Two different data processing strategies are employed to compute the gravity anomalies in the study area. The performance of the CNN technique is evaluated by comparing the results, as illustrated in Fig. 2.

In the first processing strategy, the residual DOV components of each satellite are calculated separately by along-track LSC method (Hwang and Parsons 1995), after subtracting the long-wavelength reference field and the effect of sea surface topography. Then the CNN technique is applied to each residual DOV components to determine the residual gravity in the study area. Finally, by restoring the long-wavelength gravity from EGM2008, we get the gravity anomaly model named GA_CNN.

The second processing strategy follows a common approach in gravity recovery from altimeter. Firstly, the along-track residual geoid gradients of each satellite are calculated by differentiation, after subtracting the long-wavelength reference field and the effect of sea surface topography. These residual geoid gradients are then fused using appropriate weights to compute the gridded residual DOV by LSC. The weights are determined by the precision of geoid gradients, which is derived from crossover discrepancies of SSHs after the crossover adjustment. The details followed the method proposed by Zhu et al. (2020). The residual DOV is then converted to residual gravity by IVM formula. Finally, by restoring the long-wavelength gravity from EGM2008, a gravity anomaly model named GA_IVM is obtained.

To assess the performance of CNN method, the results from both data processing approaches are compared with shipborne gravity data and other gravity models.

3.1 Data preprocessing

For altimeter data, we begin with the unifying of the reference ellipsoids of L2Ps and GDRs. Specifically, the Jason-2/GM SSHs are converted to those in WGS84 using the method described by Rapp et al. (1994) and Jin et al. (2008). To suppress the high-frequency noise caused by surface temporal variability, a Gaussian low-pass filter is applied to each altimeter SSH. The convolution window radius is identified as 7 km, considering that the distance between adjacent points of the 1 Hz along-track SSH is about 7 km. Subsequently, WGS84-based multi-satellite altimeter-measured SSHs are ready for next DOV gridding.

For shipborne gravity data, the systematic errors between each survey line should be eliminated primarily. Although the Eötvös and drift corrections have been applied to the released shipborne gravity, there may still be systematic errors between different cruises, due to the different measuring organization, instruments, and vessels and so on (Wessel and Watts 2012). To enhance the quality of shipborne gravity data, we employ the gravity anomalies from EGM2008 as a priori model for quality control. The reference ellipsoid for both the EGM2008 and shipborne gravity is WGS84. We first compute the differences between EGM2008 and the shipborne gravity data at measuring points. Then the mean and STD of these differences are counted. Gravity data with differences greater than three times STD are eliminated. If the mean value is far from 0, it indicates that there is a systematic error. And it is necessary to correct the systematic error by adding the average value to each measurement cruise. In the study area, due to the old age and poor accuracy of many shipborne gravity measurements, systematic errors of some cruises need to be eliminated segment by segment, among which the whole routes of RC2614 and KH7605 are not employed. In this study area, there are a total of 84,698 shipborne gravity observations. After quality control, about 4.49% of the observations are deleted as outliers and 80,899 points are retained for subsequent calculations.

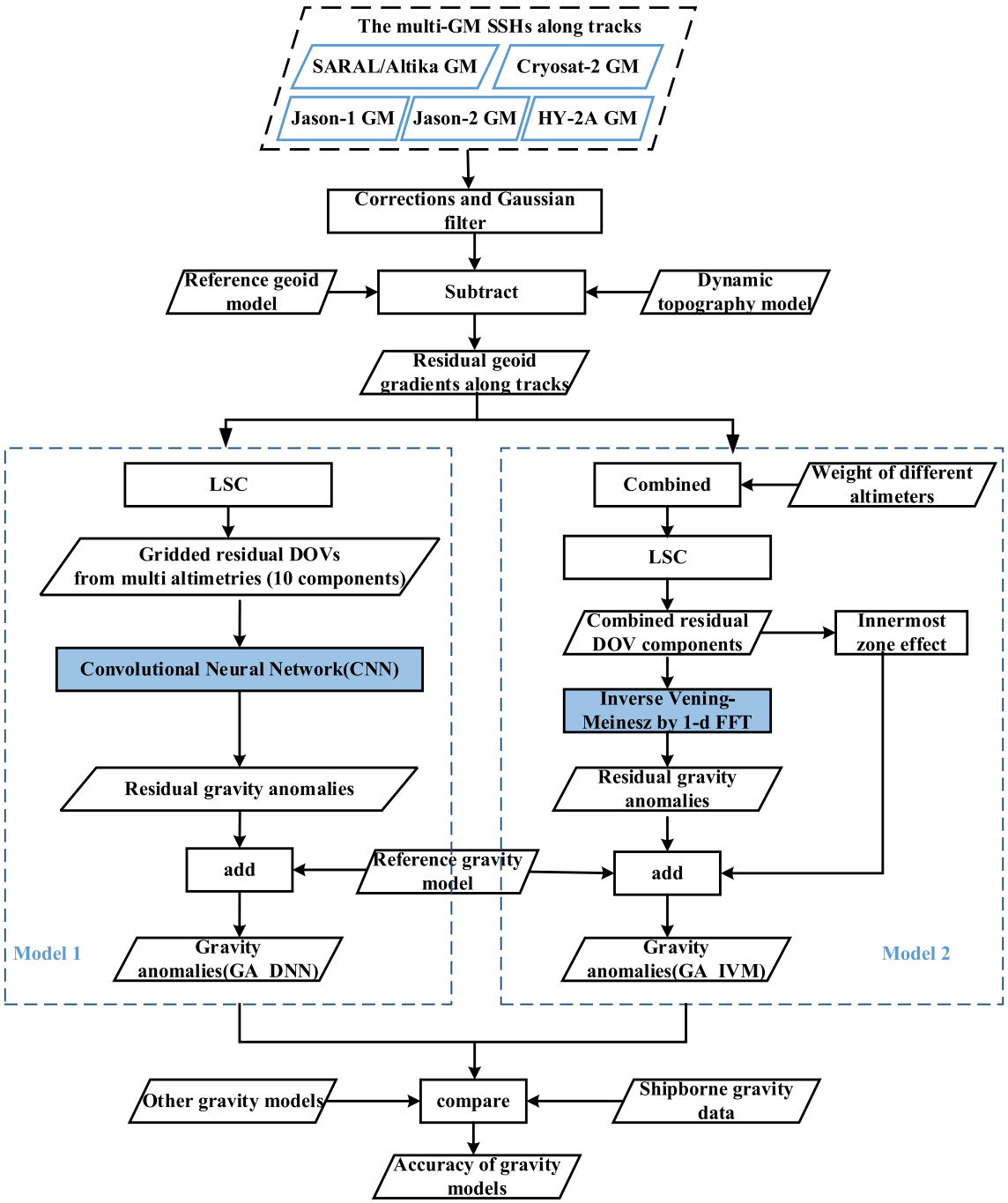

Fig. 2 The data processing strategy in this study

In addition, according to the RCR technique, the gravitational field can be divided into long-wavelength reference field and short-wavelength residual field, as shown in Eq. 1.

$$\Delta g(x,y) = \Delta g_{\mathrm{res}}(x,y) + \Delta g_{\mathrm{EGM2008}}(x,y), \tag{1}$$

where the $\Delta g_{\mathrm{res}}(x,y)$ represents the short-wavelength residual gravity field, $\Delta g_{\mathrm{EGM2008}}(x,y)$ is the long-wavelength reference gravity obtained from EGM2008.

In CNN method, the short-wavelength component of shipborne gravity at training points is employed as the feature. Before training the neural network, EGM2008 gravity anomalies at training points are subtracted from

the shipborne gravity data to obtain the residual gravity anomalies.

3.2 DOV gridding

The components of DOV are the gradients of the geoid resolved in north–south and east–west directions, which can be calculated by along-track differentiation and LSC method (Hwang and Parsons 1995). Computation of DOV through along-track differentiation can suppress long wavelength errors of SSHs and avoid the complex calculations of crossover analysis (Hwang and Parsons 1995; Zhu et al. 2020). Along-track DOV is the negative of the along-track geoid gradients, which can be calculated by differentiating the geoid of two adjacent points with respect to their spherical distance, as follows

$$e_{PQ} = -\frac{(\mathrm{SSH}_Q - \mathrm{MDT}_Q) - (\mathrm{SSH}_P - \mathrm{MDT}_P)}{\mathrm{dist}_{PQ}}, \quad (2)$$

where e_{PQ} is the along-track DOV between two adjacent points P and Q. dist_{PQ} represents the spherical distance between points P and Q. SSH_P, SSH_Q, MDT_P and MDT_Q are the adjusted SSH at points P and Q, and the sea surface topography at points P and Q from MDT-CNES-CLS18 model, respectively.

With reference to the RCR technique summarized in Fig. 2, it is a key step to calculate the residual DOV components on regular grid and use them to calculate the residual gravity anomaly. The residual DOV can be obtained by residual along-track geoid gradients, after removing the reference geoid gradients of EGM2008 from along-track geoid gradients. Then the LSC method is applied to calculate gridded residual DOV components by Zhu et al. (2020)

$$\begin{pmatrix} \xi_{\mathrm{res}} \\ \eta_{\mathrm{res}} \end{pmatrix} = \begin{pmatrix} C_{\xi e} \\ C_{\eta e} \end{pmatrix} (C_{ee} + C_{nn})^{-1} e_{\mathrm{res}}, \quad (3)$$

where e_{res} is the residual geoid gradient. η_{res} and ξ_{res} are residual east–west and north–south components of DOVs. The covariance matrices C_{ee}, $C_{\xi e}$ and $C_{\eta e}$ are for $e_{\mathrm{res}} - e_{\mathrm{res}}$, $\xi_{\mathrm{res}} - e_{\mathrm{res}}$ and $\eta_{\mathrm{res}} - e_{\mathrm{res}}$, respectively. The covariance matrices are obtained from Tscherning–Rapp degree variance Model 4 (Tscherning and Rapp 1974) and coefficients errors of EGM2008. C_{nn} is the matrix of noise variances of geoid gradients, which can be obtained by the method proposed by Hwang and Parsons (1995) and Zhu et al. (2020).

3.3 Inverse Vening Meinesz formula

Gravity anomalies can be recovered from DOVs by the IVM formula, which was presented by Hwang et al. (2002):

$$\Delta g_P = \frac{\gamma_0}{4\pi} \iint_{\sigma} H'\left(\xi_Q \cos\alpha_{QP} + \eta_Q \sin\alpha_{QP}\right) \mathrm{d}\sigma_{QP}, \quad (4)$$

where Δg_P represents the gravity anomaly at point P. γ_0 is the normal gravity based on WGS-84. η_Q and ξ_Q are the east–west and north–south components of the DOV at point Q, respectively. α_{QP} is the azimuth from Q to P. H' is the kernel function defined as

$$H'(\psi_{PQ}) = -\frac{\cos\frac{\psi_{PQ}}{2}}{2\sin^2\frac{\psi_{PQ}}{2}} + \frac{\cos\frac{\psi_{PQ}}{2}\left(3 + 2\sin\frac{\psi_{PQ}}{2}\right)}{2\sin\frac{\psi_{PQ}}{2}\left(1 + \sin\frac{\psi_{PQ}}{2}\right)}. \quad (5)$$

ψ_{PQ} is the spherical distance between Q and P. Considering that the residual components of DOVs are given in regular grid, Δg_P can be calculated by 1-D fast Fourier transform (1D FFT) (Hwang 1998). ψ_{PQ} cannot be 0, or it will cause singularity of kernel function. The innermost zone effect on gravity anomaly should be considered and are computed by $\Delta g_i = \frac{s_0\gamma_0}{2}\left(\xi_y + \eta_x\right)$, where $\xi_y = \partial\xi/\partial y$ and $\eta_x = \partial\eta/\partial x$ are the north derivative of ξ and the east derivative of η, respectively; s_0 is the radius of the innermost zone, which can be approximated from the grid intervals as: $s_0 = \sqrt{\frac{\Delta x \Delta y}{\pi}}$.

3.4 Convolutional neural network used for gravity recovery

In this study, a multilayer convolutional neural network (CNN) model is constructed to recover residual gravity using multi-altimeter DOVs and shipborne gravity. Its architecture is shown in Fig. 3. The input data is north–south and east–west components of DOVs from Altika/DP, Jason-2/GM, CryoSat-2, HY-2A/GM and Jason-1/GM, respectively, for a total of 10 components. Since the CNN input is an image, the smaller and more pixels of the image, the more it helps to extract the detailed features of the image and improve the performance of the neural network. So, each grid of DOVs is sliced into smaller grids using a 4×4 sliding window. That is the DOVs on $1' \times 1'$ grid are resampled to $0.251' \times 0.25'$. Therefore, each 4×4 grid is an equivalent of $1'$ spatial resolution. Because the gravity anomaly is an integral calculation of the DOVs in the surrounding region, employing more surrounding points provide more information for gravity determination. Considering the integration radius and the performance of computers, 32×32 surrounding points are chosen. Since the positions of the calculation points also affect the gravity field, longitude and latitude are considered as input features. All these input features are 3D-concatenated to form a 32×32×12 input image.

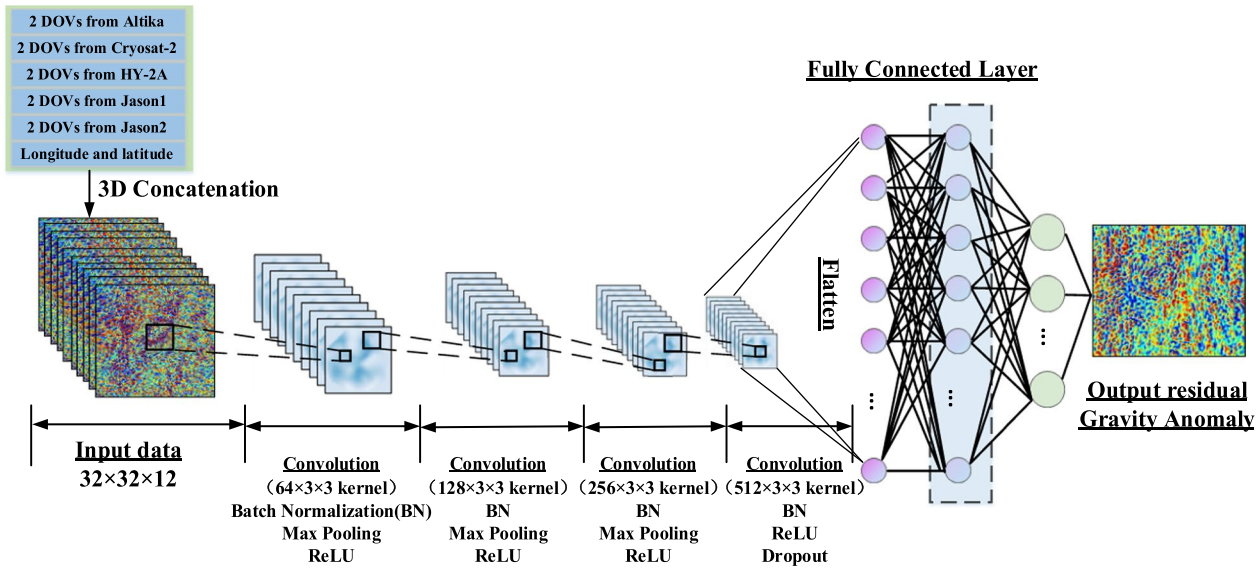

Fig. 3 CNN architecture used for gravity recovery

In addition to the input images and output result, the CNN architecture is mainly composed of seven blocks. The first three blocks are similar and consist of convolution, batch normalization, max pooling and rectified linear unit (ReLU) layers, respectively. The convolution layer conducts convolutional operations on the input images to extract features such as edges, textures and shapes. The batch normalization layer normalizes the extracted features of each layer to ensure a similar feature distribution and enhance stability. The max pooling layer reduces the dimensionality of the data and preserves the most important information. The ReLU layer applies nonlinear transformations to the output to help extract complex features. Compared to other activation functions, ReLU has stronger nonlinear fitting ability to improve the expressive power of neural network models. And it is the most commonly used nonlinear activation function (Glorot et al. 2011). The fourth block consists of convolution, batch normalization and ReLU layers, followed closely by a 25% dropout layer. The dropout layer is designed to mitigate overfitting and enhance the model's generalization capability. After flattening the extracted features, the last three blocks contain a fully connected layer with ReLU as activation function, respectively. The fully connected layers map the extracted features to the regression labels, learn the associations between the features, and implement the final regression calculation. Finally, the output of CNN is the residual gravity anomaly at the point on $1' \times 1'$ grids.

Once the neural network architecture is constructed, the important task is to train the neural network using sample data. Shipborne residual gravity with high accuracy and DOVs at training points are employed as training data, and the rest of the data is applied for testing. The neural network is trained according to the following method.

First of all, the neural network model is initialized to randomly generate initial parameters such as weights and biases. Secondly, the input data are propagated forward through the neural network architecture to obtain the output value. Thirdly, the error between the output value and the target value (testing data) is calculated, and the error is transmitted back to the network when it is larger than the expected value. The weights and biases will update according to the proper algorithm, and so on iteratively until the error meets the expected value, then the model training is completed. In this study, a loss function based on the root-mean-square error between the computed gravity and shipborne residual gravity is used to train the network for 40 epochs at an initial learning rate of 0.001. Based on the learning rate and loss function, the weights and biases are updated using Adam optimization algorithm. Adam is an algorithm for first-order gradient-based optimization of stochastic objective functions, based on adaptive estimates of lower-order moments. It can adaptively adjust the learning rate of each parameter according to the historical gradient and update of each parameter during the training process, thus speeding up the training of neural networks. Adam is widely used in large-scale neural network research (Kingma and Ba 2014). Ultimately, the derived residual gravity is

obtained by feeding the DOVs obtained from altimetry to the well-trained neural network.

4 Results and evaluation

4.1 Gravity anomalies from CNN and IVM method

Based on the data process methods described in Sect. 3 and Fig. 2, we derive two $1' \times 1'$ marine gravity models in the study area. The model calculated by CNN method is marked as GA_CNN in Fig. 4a, while the model calculated by IVM formula is marked as GA_IVM in Fig. 4b. Additionally, two gravity models used for validation, SIO V32.1 and DTU17, are also illustrated in Fig. 4c, d, under the same color bar. As demonstrated in Fig. 4, the spatial distribution of GA_CNN is highly in agreement with those of other gravity models, which clearly represents the geomorphic features such as seamounts, ridges, trenches, and submarine plains. The gravity anomalies within the entire study area range from −170 to 220 mGal, with obvious fluctuations, which are closely related to the seafloor topography. Moreover, GA_CNN and GA_IVM contain more high-frequency details compared with DTU17 and SIO V32.1. The reason may be that the V32.1 model adopts low-pass filtering related to water depth in the calculation process, cutting off the short wavelength gravity signal due to upward continuation (Sandwell et al. 2021). The DTU17 model uses geoid as data source for recovering the gravity anomalies, which contains less high-frequency information compared with DOVs.

4.2 Comparison with shipborne gravity data

To evaluate the accuracy of the GA_CNN model and the performance of the CNN method, we compare the GA_CNN model with shipborne gravity data at check points excluded from neural network training. The linear regression and differences between the GA_CNN model and the shipborne gravity are calculated, and the scatter density plot and difference distributions are represented in Fig. 5. Two main evaluation indicators are chosen to measure the linear regression: the goodness of fit R^2 and the root mean square error (RMSE). R^2 values approaching 1 indicate that the linear regression model is valid, while an RMSE close to 0 is optimal (Sun et al. 2022). In Fig. 5a, the linear regression between GA_CNN and shipborne gravity anomalies at check points yields an R^2 exceeding 0.99 and an RMSE of 3.22 mGal. All these indicate a strong correlation between the GA_CNN model and shipborne gravity. In addition, the histograms of the two gravity datasets are highly consistent, with most of the values distributed in the −30 mGal to 30 mGal range. The density plot shows that the data density is greatest in the range of 0 mGal to 5 mGal.

Figure 5b, c show the histogram and spatial distribution of differences between the GA_CNN model and shipborne gravity. The histogram result illustrates that the discrepancy values are mostly between −5 and 5 mGal, which account for 92.84% of the total, with only a few points having larger discrepancy values. The points with larger discrepancy values are mainly located in the central and eastern regions, where water depths

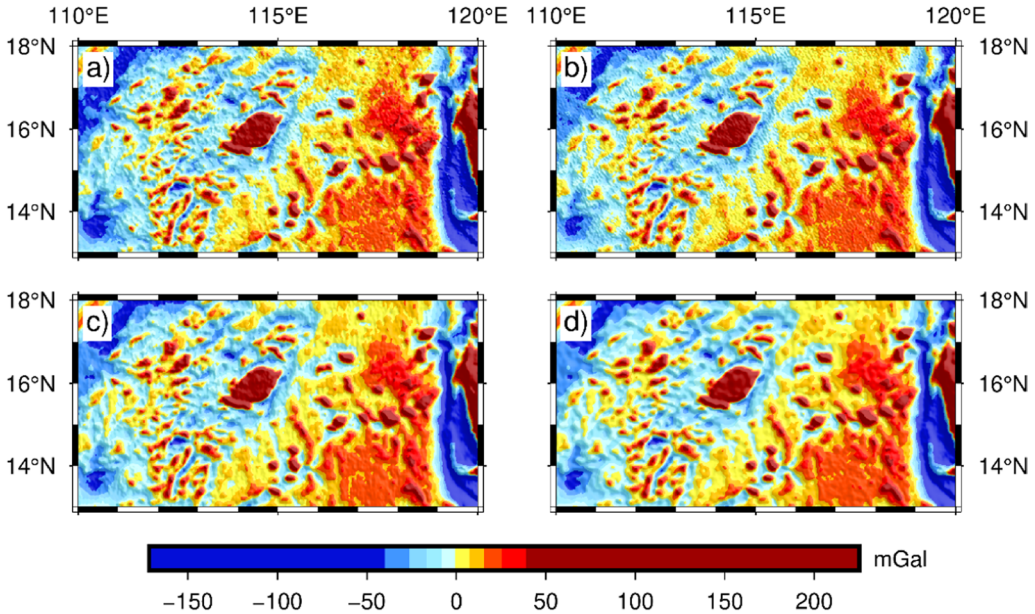

Fig. 4 Gravity models in study area. **a** GA_CNN model. **b** GA_IVM model. **c** SIO V32.1 model. **d** DTU17 model

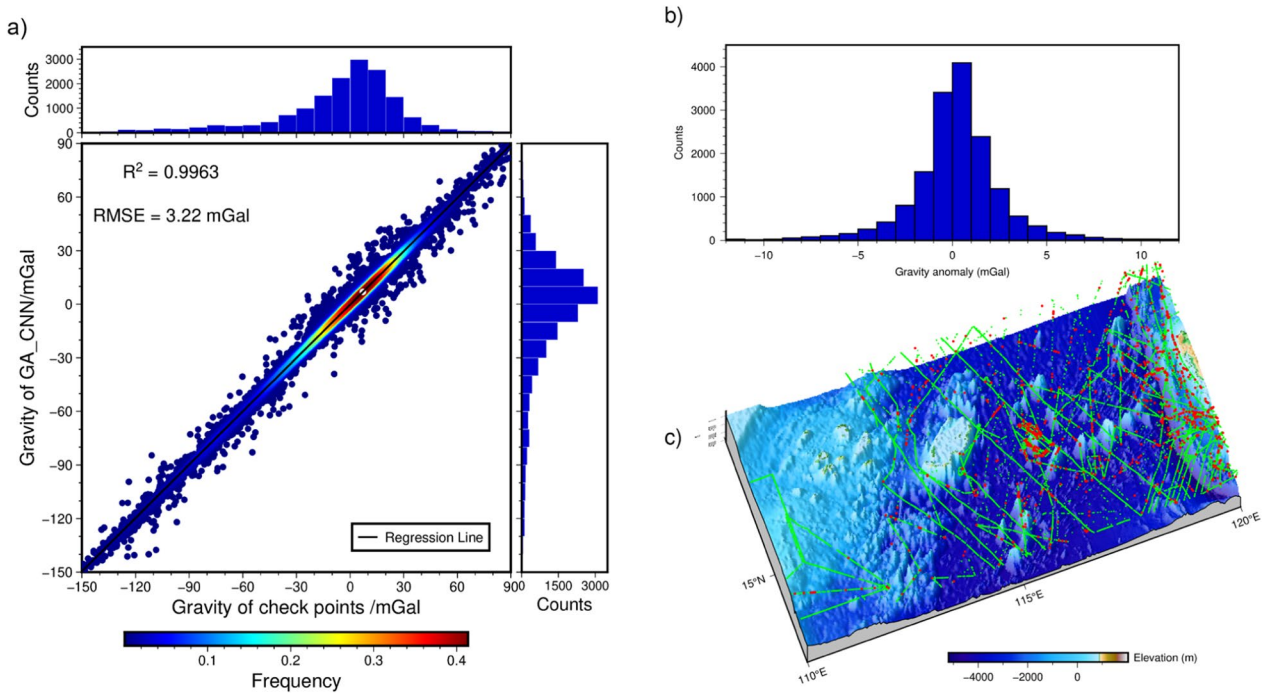

Fig. 5 The scatter density and distribution of difference between GA_CNN model and shipborne gravity at check points. **a** The scatter density between GA_CNN model and shipborne gravity, the black line is the linear regression fitting line. **b** The histogram of the differences between GA_CNN model and shipborne gravity. **c** The spatial distribution of the differences between GA_CNN model and shipborne gravity, the red dots represent points that have absolute deviations greater than 5 mGal, and the green dots show the points that have absolute deviations less than 5 mGal

Table 2 Comparisons between altimeter-derived gravity models and shipborne gravity data

Data	Max	Min	Mean	RMS	STD	Correlation Coeff. (%)
GA_CNN-shipborne	30.17	−28.36	0.22	3.22	3.21	99.63
GA_IVM-shipborne	29.80	−31.40	−0.83	5.13	5.06	99.08
V32.1-shipborne	34.38	−30.92	−0.51	4.96	4.93	99.12
DTU17-shipborne	30.33	−31.12	−0.84	5.27	5.20	99.04

Unit: mGal

are shallow and topography changes rapidly. This may be due to the fact that these areas are influenced by land and the accuracy of SSHs from multi-altimeter is relatively low, limiting the accuracy of gravity recovery. In addition, at the turning points of the ship surveying line, the discrepancy is generally large due to the effect of sharp directional changes on Eötvös correction, thus influencing the accuracy of shipborne gravity measurement. As one of the important means of marine gravity measurement, shipborne gravity measurement requires more reasonable track planning and more accurate data processing.

The deviations of GA_CNN, GA_IVM and other models from the shipborne gravity at check points

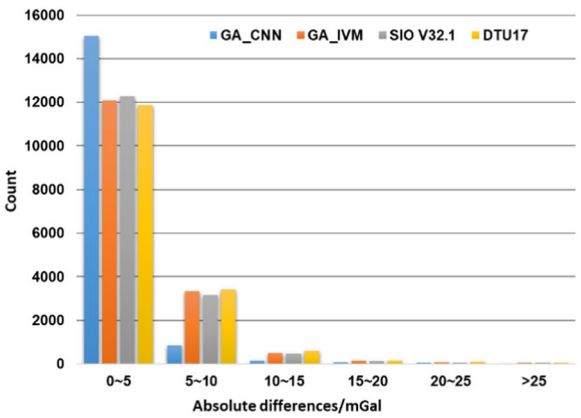

Fig. 6 The histogram distribution of the absolute differences between shipborne gravity and gravity models at check points

are computed. The STDs and correlation coefficients are shown in Table 2 and the comparison of histogram distributions is displayed in Fig. 6. For the GA_CNN model, the STD of deviation is 3.21 mGal, with an improvement of 36.56% compared to GA_IVM, 34.89% compared to SIO V32.1, and 38.27% compared to DTU17. The correlation coefficient between the GA_CNN model and shipborne gravity reaches 99.63%, surpassing that of the other models. From Fig. 6, it is evident that 92.84% of the absolute deviations between the GA_CNN model and shipborne gravity are less than 5 mGal, which is significantly higher than GA_IVM model (74.62%), SIO V32.1 model (75.90%), and DTU17 model (73.34%). These results show that the GA_CNN model achieved higher accuracy and CNN method for marine gravity recovery is feasible.

Furthermore, to analyze the actual spatial resolution of derived models, an uninterrupted marine gravity profile with higher resolution, measured by independent JMGrav marine gravimeter (Wu et al. 2023), is applied for cross spectral analysis between marine and derived altimetric gravity. The location of the marine gravity profile is presented in the top left of Fig. 7a. JMGrav marine gravimeter adopts a new gravity sensor based on electromagnetic damping, ensuring the accuracy of the gravity measurements better than 2 mGal, with approximate resolution of 500 m (Wu et al. 2023). Figure 7a displays the result of the marine and altimetric gravity profile comparisons. All four altimetric gravity models yield approximately the same profiles as the JMGrav gravity, verifying the veracity of the computed results. Table 3 provides the statistical results of difference between each altimetry-derived gravity model and JMGrav gravity. Compared to the JMGrav gravity, the GA_CNN model has an STD error of 3.17 mGal, while the other models GA_IVM, SIO V32.1 and DTU17 have STDs of 3.67, 3.54 and 3.89 mGal, respectively.

Cross-spectral analysis can measure the correlation of two signals at different wavelengths. Shipborne gravity is assumed to have high resolution due to its high sampling rate of a few meters. By cross spectrum between the interpolated altimetry and shipborne gravity profile, the actual resolution of the altimetry-derived gravity field can be analyzed (Yale et al. 1995). The cross spectrum between JMGrav gravity and interpolated altimetry gravity profiles are calculated and shown in Fig. 7b–e. The findings suggest that at short wavelengths the shipborne gravity anomalies are more powerful than altimetry-derived gravity anomalies. It is noteworthy that the GA_CNN and GA_IVM models gradually attain power comparable to shipborne gravity at wavelengths longer than approximately 7 km. Whereas the SIO V32.1 model gradually reaches the same power as shipborne gravity at wavelengths beyond about 10 km, and the DTU17 model has the same power as shipborne gravity at wavelengths beyond about 20 km. The results further show that the altimetry-derived GA_CNN and GA_IVM models have relatively higher resolution compared to SIO V32.1 and DTU17 models.

4.3 Comparison with other gravity models

To further assess the GA_CNN model, we directly compare it with the GA_IVM, SIO V32.1, and DTU17 models. We calculate the discrepancy values between the GA_CNN model and the other models, and the statistical results are shown in Table 4. The STDs of differences between the GA_CNN model and other models are between 3 and 4 mGal, which is slightly larger than that of GA_IVM model. The reason may be that GA_CNN model is quite different from the traditional inversion models over a large area in the western of the study area, as shown in Fig. 4. In these regions, the training data are sparsely distributed, whereas the CNN method relies on the amount and distribution density of the training data. This is probably making the CNN method perform worse than traditional methods. The exact conclusions need to be further verified by more independent high-precision shipborne gravity.

The power spectral density (PSD) can be used as a measure for evaluating the energy of signals at varying wavelength. Many researchers have used PSD for marine geophysical model assessment because a higher PSD indicates more details at the same wavelength (Annan and Wan 2022; Li et al. 2023; Sun et al. 2022). The PSD is computed as $10\log_{10}(P)$, where P is the relevant power. It is expressed in dB. The PSDs of the four gridded marine gravity models are shown in Fig. 8.

At medium to long wavelengths (≥ 25 km) as shown in Fig. 8, the energies of the four gravity models are comparable and relatively high. At short wavelengths less than 25 km (in red broken rectangle in Fig. 8), the energies are low. Nevertheless, the GA_CNN model generates a relatively high energy, which indicates that the GA_CNN model carries more short-wavelength gravity details than the other models. The reason may be that the GA_CNN model is derived from CNN method, which uses shipborne gravity to train the neural network model. The spatial resolution and accuracy of shipborne gravity are both relatively high, so GA_CNN contains more high-frequency signals of gravity. In addition, SIO V32.1 model adopts low-pass filtering related to water depth in the calculation process, which filters out some high-frequency information. DTU17 uses the geoid as the data source to recover gravity anomaly, and the geoid contains less high-frequency information than DOVs. It further attests that CNN method can introduce shipborne

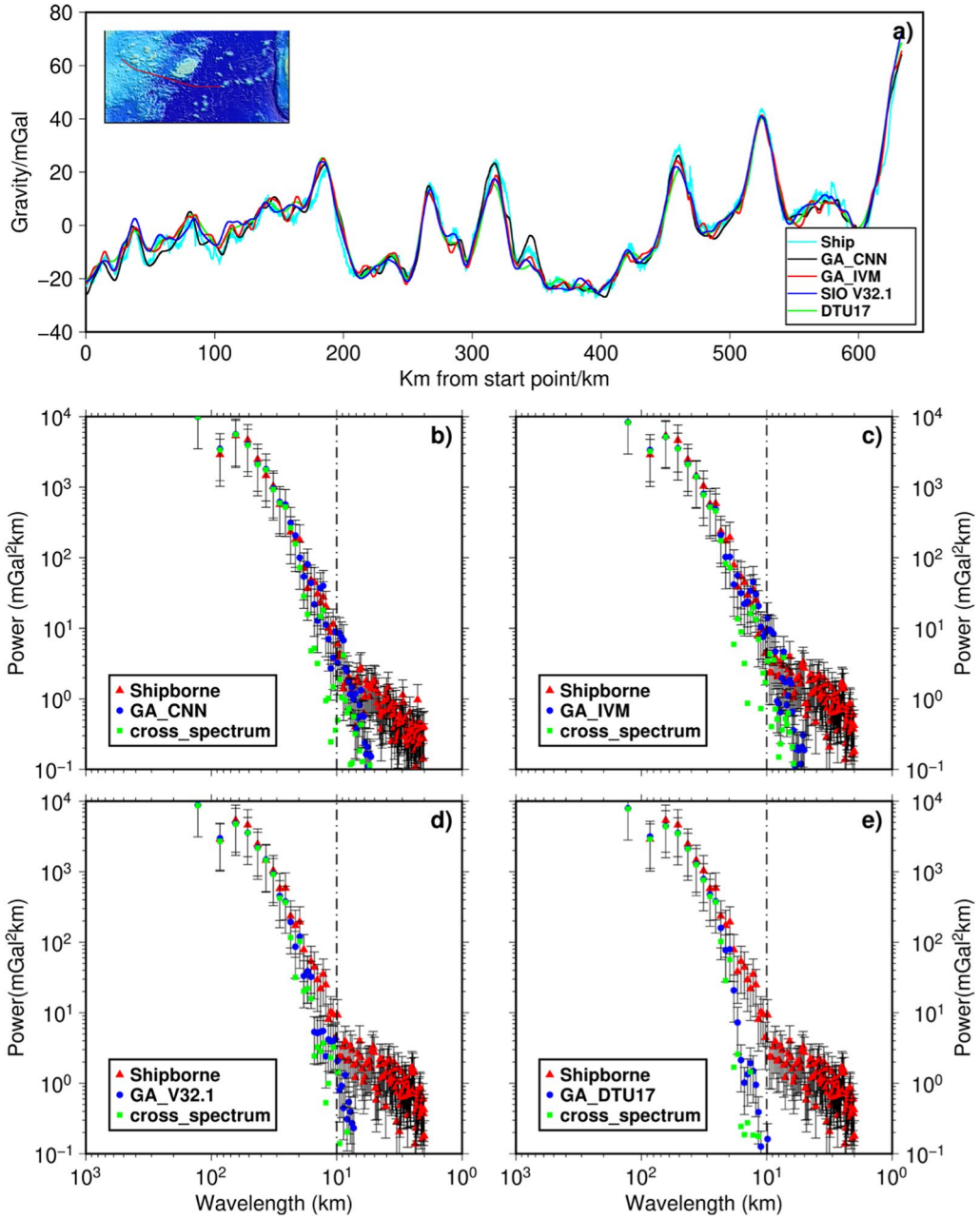

Fig. 7 The JMGrav gravity profile in study area (**a**), location of the profile is inserted in the figure to the top left. And the cross-spectral analysis of shipborne gravity and GA_CNN, GA_IVM, SIO V32.1 and DTU17, respectively (**b**–**e**)

Table 3 Comparisons between altimeter-derived gravity models and JMGrav shipborne gravity data

Data	Max	Min	Mean	RMS	STD	Correlation Coeff. (%)
GA_CNN-JMGrav	12.13	− 13.31	0.49	3.21	3.17	97.19
GA_IVM-JMGrav	12.13	− 14.20	0.11	3.67	3.67	97.31
V32.1-JMGrav	14.51	− 15.28	− 0.38	3.56	3.54	97.19
DTU17-JMGrav	13.94	− 14.92	− 0.04	3.90	3.89	97.02

Unit: mGal

Table 4 Comparisons between altimeter-derived gravity and other marine gravity models

Data	Min	Max	Mean	RMS	STD
GA_CNN-V32.1	−55.90	29.26	−0.86	4.08	3.97
GA_CNN-DTU17	−33.70	30.35	−0.94	3.98	3.88
GA_IVM-V32.1	−41.12	23.60	0.04	2.54	2.54
GA_IVM-DTU17	−15.57	14.58	−0.04	1.94	1.94
GA_CNN-GA_IVM	−33.64	31.74	−0.89	3.74	3.63
V32.1-DTU17	−20.28	37.07	−0.08	2.28	2.28

Unit: mGal

gravity as prior information reasonably to improve the accuracy and spectral characteristics of constructed gravity model.

5 Conclusions

In this study, a convolutional neural network (CNN) and remove-compute-restore (RCR) technology are applied to derive the gravity model in the SCS by combining multi-mission DOVs from Altika/DP, HY-2A/GM, CryoSat-2, Jason-2/GM and Jason-1/GM. The network's inputs are $32\times32\times12\times n$ images consisting of geo-information about the calculated point and residual DOVs on surrounding points. The output of CNN is the residual gravity anomaly at the calculated point. The final gravity anomaly is then recovered by restoring the long-wavelength reference gravity field. In addition to CNN method, gravity anomaly also be calculated by IVM formula. To assess the accuracy of the recovered gravity model and the performance of CNN method, we compare GA_CNN, GA_IVM models to independent shipborne gravity, JMGrav gravity profile and gravity anomaly models SIO V32.1 and DTU17.

The results show that the CNN method could calculate marine gravity model effectively via simplified fusion of multi-source DOVs, and the derived model reached a high accuracy level. There is a strong correlation between the GA_CNN model and shipborne gravity, with R^2 of the linear regression exceeding 0.99. The STD of the differences between the GA_CNN model and shipborne gravity is 3.21 mGal, with significantly improvement than GA_IVM model of 5.06 mGal, the SIO V32.1 model of 4.93 mGal, and the DTU17 model of 5.20 mGal. More than 92% of the absolute differences between the GA_CNN model and shipborne gravity are less than 5 mGal. The STD between the GA_CNN model and JMGrav gravity profile is 3.17 mGal, which is superior to all other models. The correlation coefficients between the GA_CNN model and the other gravity models exceed 99%, indicating that the GA_CNN model is largely consistent with other gravity models. Furthermore, the PSDs of four gravity models are also computed and compared. The results show that the GA_CNN model has stronger energy at short wavelength (less than 25 km) than other models, which suggests that CNN method can introduce

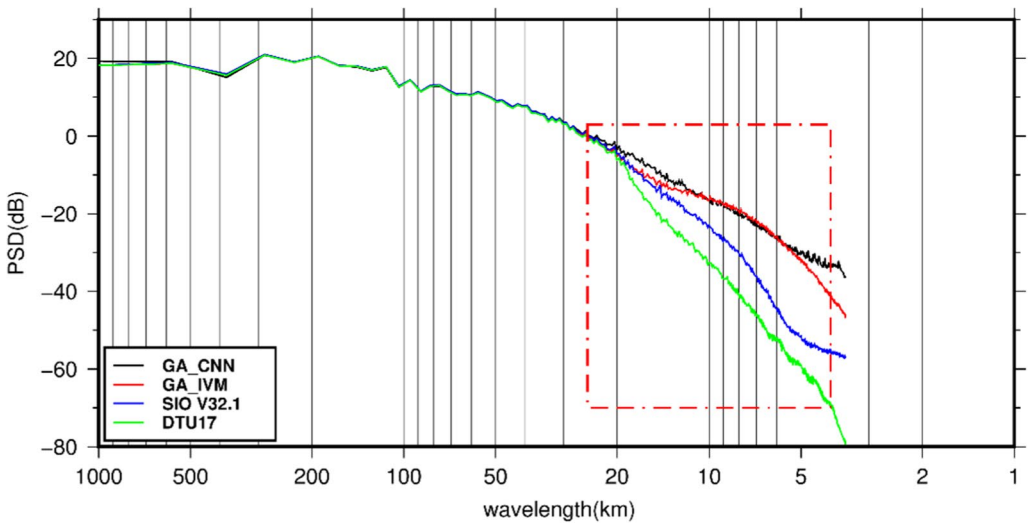

Fig. 8 PSD of gravity models. The black line represents the PSD of the CNN-derived model, the red line represents the IVM-derived model, the blue line represents the V32.1 model, and the green line represents the DTU17 model. The red broken rectangle indicates the wavelengths less than 25 km

shipborne gravity as prior information reasonably to improve the accuracy and spectral characteristics of constructed gravity model.

Abbreviations

CNN	Convolutional neural network
DOVs	Vertical deflections
IVM	Inverse Vening Meinesz
STD	Standard deviation
SSHs	Sea surface heights
LSC	Least squares collocation
GMs	Geodetic missions
T/P	TOPEX/POSEIDON
RCR	Remove–compute–restore
AltiKa/DP	SARAL/AltiKa/Drifting Phase
SCS	South China Sea
L2P	Level-2 Plus
GDRs	Geophysical data records
MDT	Mean dynamic topography
EGM2008	Earth Gravitational Model 2008
NCEI	National Centers for Environmental Information
SIO	Scripps Institution of Oceanography
DTU	DTU space
1D FFT	1-D fast Fourier transform
ReLU	Rectified linear unit
RMSE	Root mean square error
PSD	Radially power spectral density

Acknowledgements
We are grateful to the anonymous reviewers for constructive reviews that improved the manuscript greatly. This research is funded by the National Natural Science Foundation of China (Grant Nos. 41931076, 42192535, 42174102) and the Natural Science Foundation of Hubei Province (2022CFB816).

Author contributions
LB, QL and HS conceived this study and designed the experiments. QL and ZZ carried out the experiments and wrote the initial draft of the manuscript. LB, YW, LW, GM and HS analyzed the results and revised the manuscript. All authors read and approved the final manuscript.

Funding
This research is funded by the National Natural Science Foundation of China (Grant Nos. 41931076, 42192535, 42174102) and the Natural Science Foundation of Hubei Province (2022CFB816).

Availability of data and materials
The L2P products for missions Jason-2, Jason-1, SARAL/AltiKa, Crysoat-2, HaiYang-2A and the GDR products of Jason-3 are available at AVISO+ (https://www.aviso.altimetry.fr/). The shipborne gravity data are provided by the National Centers for Environmental Information (NCEI, https://www.ncei.noaa.gov/) and SeaDataNet Pan-European infrastructure for ocean and marine data management (https://www.seadatanet.org). The altimeter-derived gravity anomaly models V32.1 and DTU17 used in this study are obtained from University of California at San Diego (ftp://topex.ucsd.edu/) and DTU Space, f: https://www.space.dtu.dk/.

Declarations

Competing interests
The authors declare that they have no known competing financial interests or personal relationships that could have appeared to influence the work reported in this paper.

Author details
[1]State Key Laboratory of Geodesy and Earth's Dynamics, Innovation Academy for Precision Measurement Science and Technology, Chinese Academy of Sciences, Wuhan 430077, China. [2]State Key Laboratory of Geo-Information Engineering, Xi'an Research Institute of Surveying and Mapping, Xi'an 710054, China. [3]University of Chinese Academy of Sciences, Beijing 100049, China. [4]School of Geography and Information Engineering, China University of Geosciences (Wuhan), Wuhan 430074, China.

Received: 25 April 2024 Accepted: 18 September 2024
Published online: 11 October 2024

References

Andersen OB, Knudsen P (1998) Global marine gravity field from the ERS-1 and Geosat geodetic mission altimetry. J Geophys Res Oceans 103(C4):8129–8137. https://doi.org/10.1029/97jc02198
Andersen OB, Knudsen P (2019) The DTU17 global marine gravity field: first validation results. Fiducial reference measurements for altimetry. Springer, Cham, pp 83–87
Andersen OB, Knudsen P, Berry PAM (2010) The DNSC08GRA global marine gravity field from double retracked satellite altimetry. J Geodesy 84(3):191–199. https://doi.org/10.1007/s00190-009-0355-9
Andersen OB, Zhang S, Sandwell DT, Dibarboure G, Abulaitijiang A (2021) The unique role of the Jason geodetic missions for high resolution gravity field and mean sea surface modelling. Remote Sens 13(4):646
Annan RF, Wan X (2022) Recovering bathymetry of the gulf of guinea using altimetry-derived gravity field products combined via convolutional neural network. Surv Geophys 43(5):1541–1561. https://doi.org/10.1007/s10712-022-09720-5
CNES (2020) Along-track level-2+ (L2P) SLA product handbook. https://www.aviso.altimetry.fr/fileadmin/documents/data/tools/hdbk_L2P_all_missions_except_S3.pdf. Accessed 20 Dec 2023
Dong X, Zhong T, Li Y (2020) A deep-learning-based denoising method for multiarea surface seismic data. IEEE Geosci Remote Sens Lett 18(5):925–929
Forsberg R (1984) A study of terrain reductions, density anomalies and geophysical inversion methods in gravity field modelling. Report 355, Dept. of Geod. Sci. and Surv., Ohio State University, Columbus
Glorot X, Bordes A, Bengio Y (2011) Deep sparse rectifier neural networks. J Mach Learn Res 15:315–323
Haxby WF, Karner GD, LaBrecque JL, Weissel JK (1983) Digital images of combined oceanic and continental data sets and their use in tectonic studies. EOS Trans Am Geophys Union 64(52):995–1004. https://doi.org/10.1029/EO064i052p00995
Hwang C (1998) Inverse Vening Meinesz formula and deflection-geoid formula: applications to the predictions of gravity and geoid over the South China Sea. J Geod 72(5):304–312. https://doi.org/10.1007/s001900050169
Hwang C, Parsons B (1995) Gravity anomalies derived from Seasat, Geosat, ERS-1 and TOPEX/POSEIDON altimetry and ship gravity: a case study over the Reykjanes Ridge. Geophys J Int 122(2):551–568. https://doi.org/10.1111/j.1365-246X.1995.tb07013.x
Hwang C, Hsu HY, Jang RJ (2002) Global mean sea surface and marine gravity anomaly from multi-satellite altimetry: applications of deflection-geoid and inverse Vening Meinesz formulae. J Geod 76(8):407–418. https://doi.org/10.1007/s00190-002-0265-6
Jin TY, Li JC, Xing LL, Chu YH (2008) Research on datum unification of multi-satellite altimetric data. J Geod Geodyn 03:92–95+99 (**in Chinese**)
Kingma DP, Ba J (2014) Adam: a method for stochastic optimization. arXiv preprint. https://arxiv.org/abs/1412.6980
Li Q, Zhai Z, Li Q, Wu L, Bao L, Sun H (2023) Improved bathymetry in the South China Sea from multisource gravity field elements using fully connected neural network. J Mar Sci Eng 11(7):1345. https://doi.org/10.3390/jmse11071345
Olgiati GB, Sarrailh M, Green CM (1995) Gravity anomalies from satellite altimetry: comparison between computation via geoid heights and via defections of the vertical. Bull Géodésique 69(4):8
Pavlis NK, Holmes SA, Kenyon SC, Factor JK (2012) The development and evaluation of the Earth Gravitational Model 2008 (EGM2008). J Geophys Res Solid Earth. https://doi.org/10.1029/2011jb008916
Perol T, Gharbi M, Denolle M (2018) Convolutional neural network for earthquake detection and location. Sci Adv 4:e1700578
Rapp RH, Yi Y, Wang YM (1994) Mean sea surface and geoid gradient comparisons with topex altimeter data. J Geophys Res Oceans 99(C12):24657–24667

Sandwell DT, Smith WHF (1997) Marine gravity anomaly from Geosat and ERS-1 satellite altimetry. J Geophys Res Solid Earth 102:15
Sandwell DT, Smith WHF (2009) Global marine gravity from retracked Geosat and ERS-1 altimetry: ridge segmentation versus spreading rate. J Geophys Res Solid Earth. https://doi.org/10.1029/2008jb006008
Sandwell DT, Muller RD, Smith WH, Garcia E, Francis R (2014) Marine geophysics. New global marine gravity model from CryoSat-2 and Jason-1 reveals buried tectonic structure. Science 346(6205):65–67. https://doi.org/10.1126/science.1258213
Sandwell DT, Harper H, Tozer B, Smith WHF (2021) Gravity field recovery from geodetic altimeter missions. Adv Space Res 68(2):1059–1072. https://doi.org/10.1016/j.asr.2019.09.011
Sun H, Feng Y, Fu Y, Sun W, Peng C, Zhou X, Zhou D (2022) Bathymetric prediction using multisource gravity data derived from a parallel linked BP neural network. J Geophys Res Solid Earth 127:e2022JB024428. https://doi.org/10.1029/2022JB024428
Tscherning CC, Rapp HR (1974) Closed covariance expressions for gravity anomalies, geoid undulations, and deflections of the vertical implied by anomaly degree variance models. Reports of the Department of Geodetic Science. No. 208. The Ohio State University, Columbus
Wang YM (1999) On the ellipsoidal corrections to gravity anomalies computed using the inverse Stokes integral. J Geod 73:5
Wessel P, Watts AB (2012) On the accuracy of marine gravity measurements. J Geophys Res Solid Earth 93(B1):393–413. https://doi.org/10.1029/JB093iB01p00393
Wu P, Wu L, Bao L, Wang L, Wang B, Tang D (2023) A marine gravimeter based on electromagnetic damping and its tests in the South China Sea. J Oceanol Limnol 41(2):792–803
Yale MM, Sandwell DT, Smith WHF (1995) Comparison of along-track resolution of stacked Geosat, ERS 1, and TOPEX satellite altimeters. J Geophys Res Solid Earth 100(B8):15117–15127
Yu D, Hwang C (2022) Calibrating error variance and scaling global covariance function of geoid gradients for optimal determinations of gravity anomaly and gravity gradient from altimetry. J Geod 96(9):61. https://doi.org/10.1007/s00190-022-01647-4
Yu D, Hwang C, Andersen OB, Chang ETY, Gaultier L (2021) Gravity recovery from SWOT altimetry using geoid height and geoid gradient. Remote Sens Environ 265:112650. https://doi.org/10.1016/j.rse.2021.112650
Zhang S, Sandwell DT, Jin T, Li D (2017) Inversion of marine gravity anomalies over southeastern China seas from multi-satellite altimeter vertical deflections. J Appl Geophys 137:128–137. https://doi.org/10.1016/j.jappgeo.2016.12.014
Zhang S, Abulaitijiang A, Andersen OB, Sandwell DT, Beale JR (2021) Comparison and evaluation of high-resolution marine gravity recovery via sea surface heights or sea surface slopes. J Geod 95(6):66. https://doi.org/10.1007/s00190-021-01506-8
Zhao Y, Li Y, Dong X, Yang B (2018) Low-frequency noise suppression method based on improved DnCNN in desert seismic data. IEEE Geosci Remote Sens Lett 16(5):811–815
Zhu C, Guo J, Gao J, Liu X, Hwang C, Yu S, Yuan J, Ji B, Guan B (2020) Marine gravity determined from multi-satellite GM/ERM altimeter data over the South China Sea: SCSGA V1.0. J Geod 94(5):1–16. https://doi.org/10.1007/s00190-020-01378-4
Zhu C, Yang L, Bian H, Li H, Guo J, Liu N, Lin L (2023) Recovering gravity from satellite altimetry data using deep learning network. IEEE Trans Geosci Remote Sens 61:1–11. https://doi.org/10.1109/tgrs.2023.3280261

Publisher's Note